Width Increased Dual-Pump Coherent Anti-Stokes Raman Spectroscopy (WIDECARS) Setup Report at DLR-VT-Stuttgart

Dr. Luca M. L. Cantu

Luca.Cantu@dlr.de
+49 (0) 711 / 6862 257

DLR Stuttgart
Institute of Combustion Technology
Combustion Diagnostics Department

Deutsches Zentrum
DLR für Luft- und Raumfahrt

Document properties

Title	WIDECARS Setup Report at DLR-VT-Stuttgart
Subject	Laser diagnostics development
Institute	Institute of Combustion Technology – Combustion Diagnostics Department
Created by	Dr. Luca M. L. Cantu
Date	Aug 2019
Version	1.0

Index

1. Introduction

Coherent Anti-Stokes Raman Spectroscopy (CARS)[1,2] is a non-linear spectroscopic technique that provides spatially and temporally resolved temperatures and species concentrations by probing molecular Raman shifts. Three coherent laser beams (pump, Stokes and probe) are focused and crossed in the region of interest generating a CARS signal beam as shown in Figure 1. The frequencies of the three beams are chosen such that their interaction excites the molecular vibrational transitions of the N_2 Q-branch. In broad-band vibrational CARS the probe beam has a broad bandwidth that covers several vibrational and rotational transitions of the molecule.

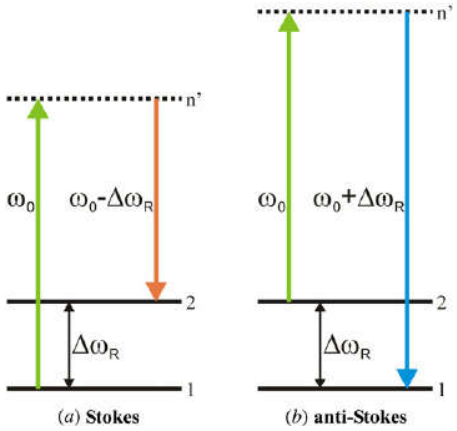

Figure 1. CARS energy level diagram (source: M. C. Weikl)

The resulting signal beam carries the Raman spectra of N_2. Processing of the spectra allows temperature to be obtained by fitting the spectral shape. In broadband vibrational CARS, a spectrum is obtained with each single laser shot and the temperature distribution (probability density function, pdf) is obtained from the measurement of a large number of single spectra. The temperature pdfs carry important information about the combustion process. The Shifted Vibrational (SV) CARS is a different arrangement that employs a narrow-band dye laser in place of the 532 nm laser to shift the CARS signal from the often used 473 nm to 519 nm as shown in Figure 2.[3] This arrangement avoids interference due to laser-induced C_2 emissions.[4]

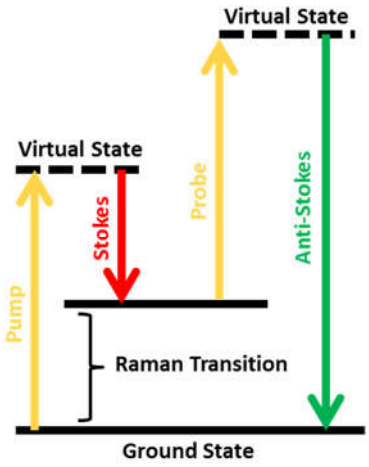

Figure 2. SV-CARS energy level diagram

A further development is the employment of dual-pump (DP) CARS.[5] In this different arrangement three lasers are employed: two narrow band dye lasers and a broad band dye laser. Pump and probe beams exchange roles during the measurement to detect simultaneously two different Raman shifts (in this case, in the vicinity of N_2 and O_2 resonances), as shown in Figure 3. Choosing carefully the frequencies of the probe beam and the Stokes beam provides a signal that is not disturbed by the Swan band interference[6].

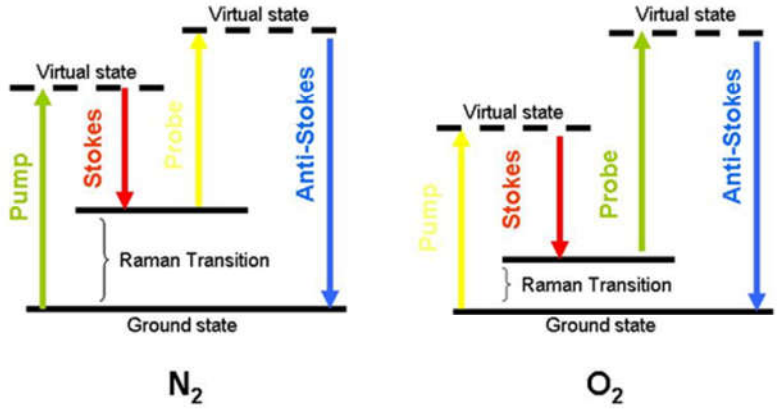

Figure 3. DP-CARS energy level diagrams for N_2 and O_2 (source: L. M. L. Cantu)

A further advancement is the employment of the Width Increased Dual-pump Enhanced (WIDE) CARS proposed initially by Flores,[7] then by Tedder et al.[8] and modified and optimized by Gallo et al.[9,10] shown in Figure 4.

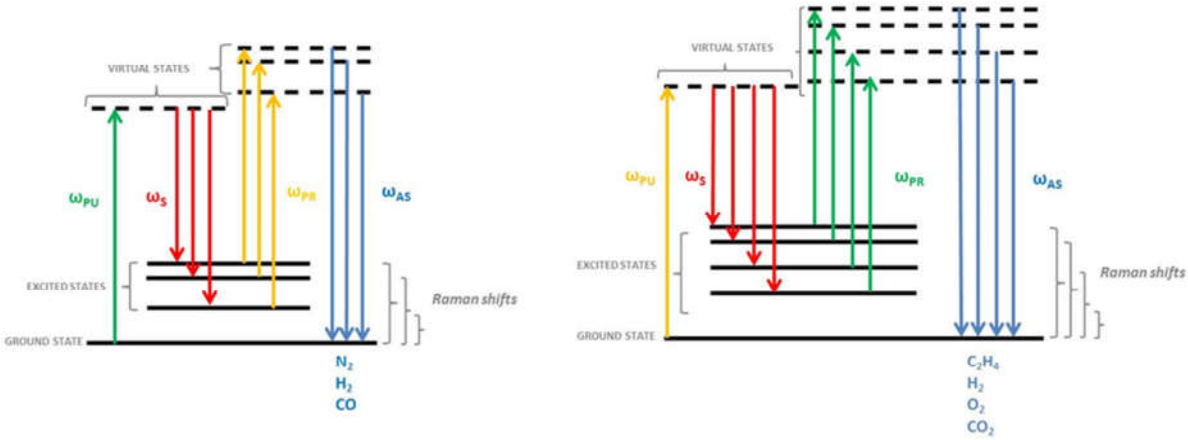

Figure 4. WIDECARS energy level diagrams for C_2H_4, N_2, O_2, H_2, CO, CO_2 (source: E. C. A. Gallo)

The advantage of WIDECARS is the capability to probe multiple specie concentrations (C_2H_4, N_2, O_2, H_2, CO, CO_2) simultaneously with temperature due to the uncommon broad broad-band dye laser. Usually a Full Width Half Max (FWHM) of at least 16 nm is required to be able to probe all the desired species. This technique is particularly attractive in combustion environment where all the major specie concentrations are measured and the main product (H_2O) could be derived by difference under appropriate assumptions.[11]

2. Optical setup upgrade inside the SV-CARS container

The SV-CARS container at DLR Stuttgart was setup to perform only temperature measurements out of N_2 spectra. The optical setup was modified in order to deliver a dual pump CARS configuration. The major change was performed on the narrow-band dye laser line to obtain an additional laser path for the 532 nm laser. The basic idea was to build the 532 nm line taking out portion of the pumping beam of the narrow-band dye laser. Two are the reasons for this choice: first of all, the narrow-band dye laser was not split in two different paths after the beam attenuator. Having just a single beam delivered for the measurement allowed affording a small decrease in energy due to a lower energy pumping beam. Secondly the broad-band dye laser is the most sensitive to changes component in the WIDECARS setup, so modifying the pumping beam or changing the laser path may have led to extra efforts to re-configure the system. So, a 90:10 beam splitter was placed in the narrow-band dye laser pump beam path: 10% of the pumping beam (~25 mJ/pulse) was used to create the 532 nm laser path while the remaining 90% continued on the original path and pumped the oscillator and amplifier dye cells of the narrow-band dye laser. Figure 5 shows the SV-CARS (a) and WIDECARS (b) setup.

Other optical changes and updates were made at the exit of the dye lasers.
All the optical components used previously to perform Laser Induced Incandescence (LII) and all the optics used to attempt Laser Induced Fluorescence (LIF) in 2015 were removed (March 2018) and stored in the appropriate optical cabinets or returned to the respective laboratory supervisors. This was due to create enough space to setup the 532 laser path, delay line and beam attenuator (replaced half-wave plate in May 2018) since it was not possible to use the removed laser paths anymore; the original Nd:YAG laser (*Spectra Physics Quanta Ray GCR 230*) failed in June 2016 and replaced with a similar model (*Spectra Physics Quanta Ray GCR 210-10*) in August 2016. However, the housing of the replacing laser was slightly different and it was not possible to setup again the 1064 nm line used for the LII system due to lack of space (an amplifier cell is the space of the previous delivering optics).
Regarding the narrow-band dye laser path, the 50:50 beam splitter originally used to create the pump and the probe beams for SV-CARS (Figure 2) was removed (April 2018). This was done to allow the 532 nm beam to use a similar laser path and minimize the alignment and optical changes. All the mirrors were replaced to maximize the transmission according to the laser wavelength in use.
On 532 nm laser path a telescope was built (August 2018) in order to control the beam diameter size and to adjust the focusing at the measurement location.
Other small changes were also done on all the three laser paths (e.g. mirror position, telescope adjustment, etc...) in order to minimize the alignment procedure, optimize the phase matching and signal intensity and simplify the alignment effort outside the laser container.

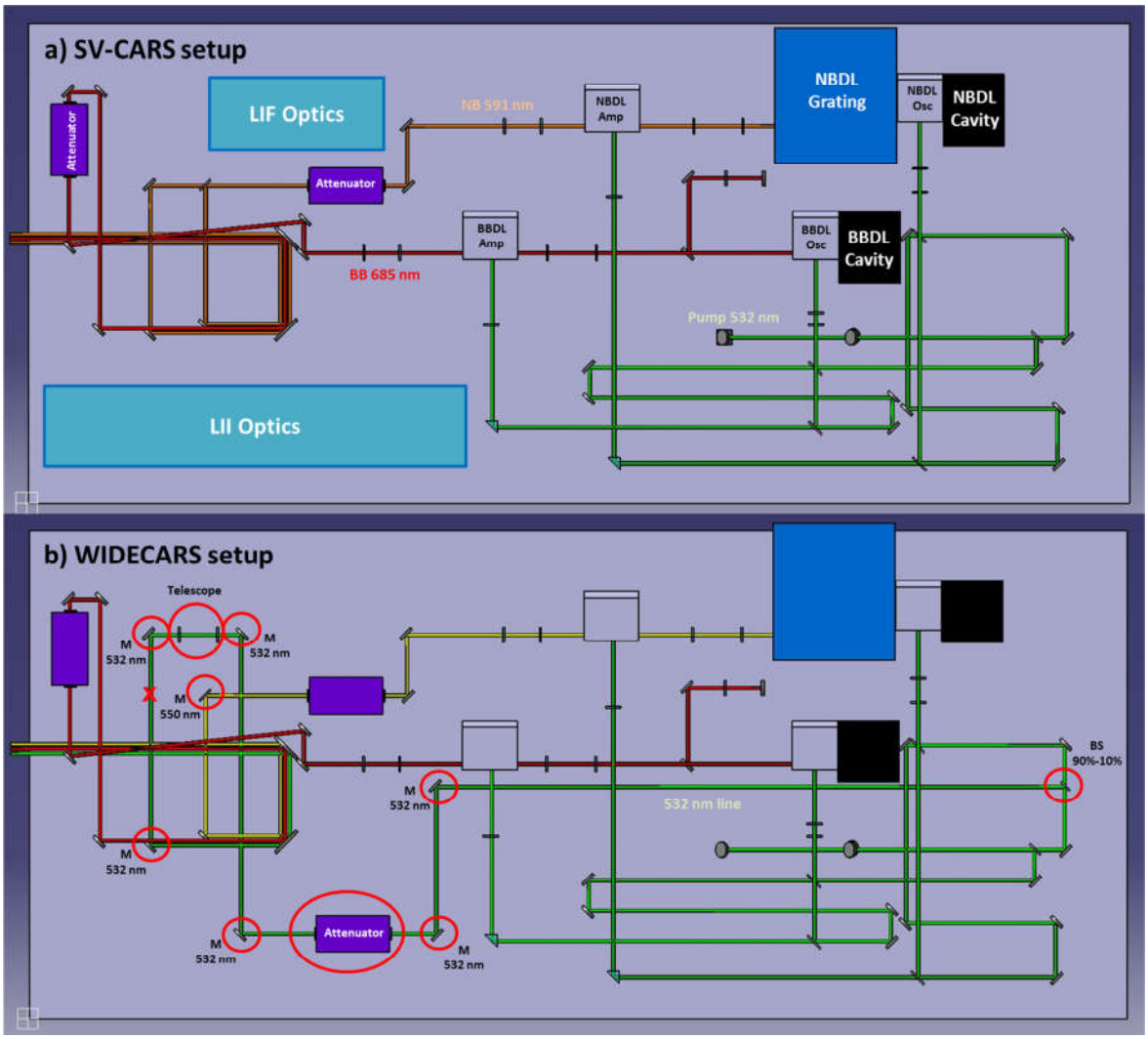

Figure 5. a) SV-CARS setup: all the main components are labeled; **b)** WIDECARS setup: all the reported changes are remarked

In addition, it is important to notice that both SV-CARS and WIDECARS system can coexist in the same laser container and a big effort was conducted to provide the capability to switch from one configuration to another with minimal adjustments. Except by the day change (both narrow-band and broad-band), the only optical component involved in the switch are only two: a 50:50 beam splitter and a mirror. Both these optical components are found on the narrow-band laser path right after the beam attenuator. Both must be removed to switch from SV to WIDECARS and put back in place to switch the system back. In addition, as described before, a high reflectance mirror must replace the 50:50 beam-splitter.

3. Broad-band dye laser modification

The most sensitive component of the WIDECARS system is the broad-band dye. The broader is the FWHM the higher is the number of chemical species that is possible to detect. So the choice of the dye is very important. However, there are several limitations to the choice of the dye. First of all safety: most of the dyes which are not in the Rhodamine family are highly cancerogenic or can cause serious health hazard. Handle the dye very carefully is a must and all the solutions must be performed under a chemical fume hood using the appropriate protections: always refer to the Material Safety Data Sheet (MSDS) prior to handle a new dye or a different solvent. The other limitation is due to the C_2 Swan band interference. The CARS signal must avoid this region limiting the possible combination of wavelengths. Moreover, while the narrow-band dye laser can be tuned to different wavelengths, the 532 nm cannot be changed. This is a further limitation because the CARS signal must be outside the Swan band but the choice of the wavelengths must probe the desired Raman shifts of the major species in combustion. The typical values of CARS signal are reported in Figure 6 overlapped to the C_2 interference.

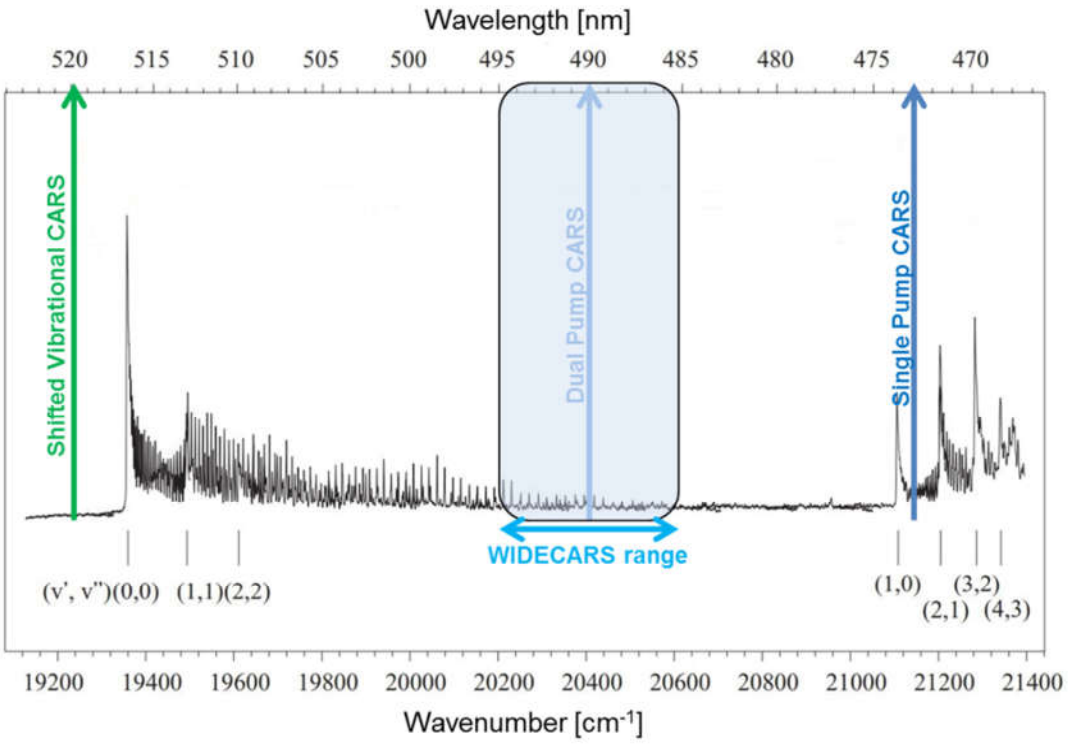

Figure 6. CARS signal overlapped to C_2 Swan band interference (source: Y. Schneider-Kühnle)

It can be noticed that the single pump CARS is not suitable for sooting flames measurements while DP-CARS and WIDECARS may face some small interference if the broad-band and narrow-band frequencies are chosen carefully. The optimal solution to meet all the above mentioned

requirements is to have a frequency of the narrow-band dye laser in the range of 550 nm and a broad-band dye laser with the peak of intensity in the range of 600 nm. This combination, coupled with the 532 nm laser beam provides a peak of the CARS signal centered in the range of 590 nm. Moreover, this frequency arrangements allows to space the chemical species far enough to minimize overlapping.

In literature[12,13,14,15] there are few dyes which can provide the desired FWHM by themselves but unfortunately their frequency range is outside the desired Raman shifts to probe: they all lie too far in the red or too far in the blue. Figure 7 is given as example: a mixture of DCM dye in Ethanol solution provides a FWHM of ~15 nm but the peak is centered at 630 nm. It is too far from the desired wavelength and any attempt to shift it towards the yellow (hence, diluting the concentration) resulted in a dramatic drop in energy.

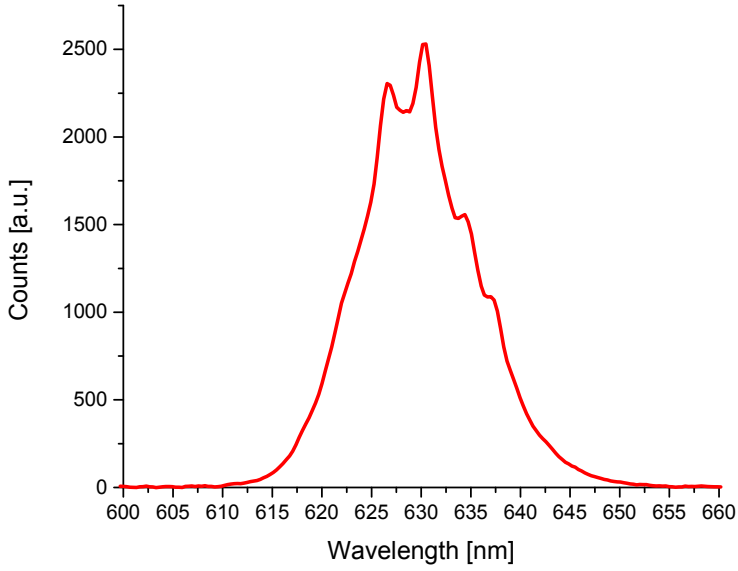

Figure 7. DCM dye in ethanol solvent

The only possible compromise is to find a dye mixture. Unfortunately not all the dye mix well together. For example: a mixture of Rhodamine dyes[9] lead only to a spectral shift without any significant increase (or decrease) of the FWHM. A mixture of Pyrromethene (597 and 650) is suggested by Flores[7] and Tedder[8]. However, the lifetime of the dye is very short, and despite the optimization made by Gallo[9] a new dye is required every 2-3 days of continuous operation. In addition, Gallo discovered in her dissertation[9] that the dye stability is influenced by several factors including dye concentration, dye temperature, frequency of the pumping beam, energy of the pumping beam, mass flow rate provided by the dye pump, dye cell geometry and laser cavity geometry. This makes every system unique and a new dye study should be performed. In addition, Pyrromethene is highly cancerogenic and it is not soluble in water, hence it is hard to be washed in case of a spill: this makes this component not desirable to work with on daily basis.

A different promising mixture is suggested by *Exciton*[13]: DCM and Sulphurhodamine 640 (or 101). The FWHM should be in the order of >20 nm with the peak of the dye around 606 nm. The main advantage is that, even though DCM is as much cancerogenic as Pyrromethene, the solution has a very long lifetime, comparable to Rhodamine dyes. The main drawback is that Sulphurhodamine dyes are very fragile and decomposition of the dye by pump radiation may cause serious damage of the dye cell, according to Sirah service manual.[15]
A good compromise between CARS signal wavelength requirement, safety, dye system integrity and dye lifetime was found mixing DCM, Rhodamine 640 and Kiton Red. Figure 8 shows the broad-band dye profile recorded with a USB spectrometer (*AVASpec-2048-USB2*).

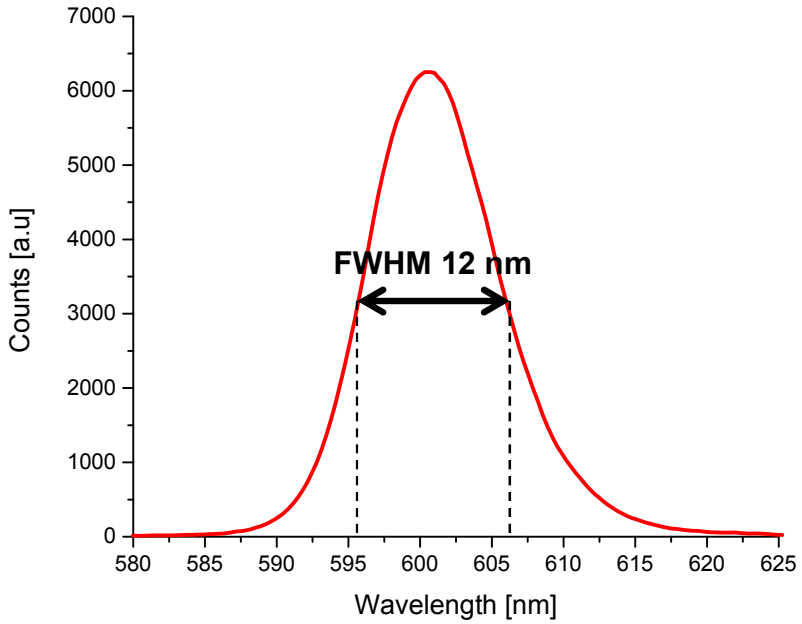

Figure 8. Mixture of DCM, Rhodamine 640 and Kiton Red dyes in ethanol solvent

The peak of the curve is centered to the desired wavelength but the FWHM is just 12 nm. However, during a demonstration test the dye curve was able to fill the entire CCD of the actual camera in use (*LaVison FlameStar2*). So no further study was conducted on the broad-band dye laser because of time restriction due to an incoming measurement campaigns (*SOPRANO Project* and *JETSCREEN project*). Moreover any additional improvement would have fallen outside the field of view of the detection system. A possible solution would have been changing the actual grating (1800 grooves per mm) inside the spectrometer with one with less dispersion (1200 or less grooves per mm). However this solution would have worsened the dispersion of the signal resulting in or unresolved spectral structures or in overlapping species.
In conclusion, the actual broad-band dye was optimized for the actual system in use, but in future further investigation is highly recommended, particularly with the upgrade of a new detection system like a *LaVision NanoStar* or with another device with similar features.

4. Spatial resolution calculation

Before setting up a test case, the spatial resolution of the WIDECARS system was tested in the Soot Lab. A tiny glass plate (thickness less than 0.2 mm) was mounted at the crossing point of the here laser beams. Two independent 3-axis translation stages moved the transmitting and the collecting optics around the measurement location. When the beams hit the glass plates it generates the non-resonant spectrum which is collected into the spectrometer and recorded on the ICCD camera. Moving the translation stage in the beam-wise direction changed the intensity of the signal determining the spatial resolution of the system. The WIDECARS phase matching was reached using the exiting folded BOXCARS configuration[3] and the three beams were focused to the measurement point through a 250 mm focal length lens. Each measurement point consisted in an average of 100 single shots and it was recorded every 0.2 mm step. The spatial resolution was calculated between 2.5% and 97.5% of the collected CARS signal. The test was repeated 3 times for repeatability purpose and the results averaged. Figure 9 shows the result of the spatial resolution test.

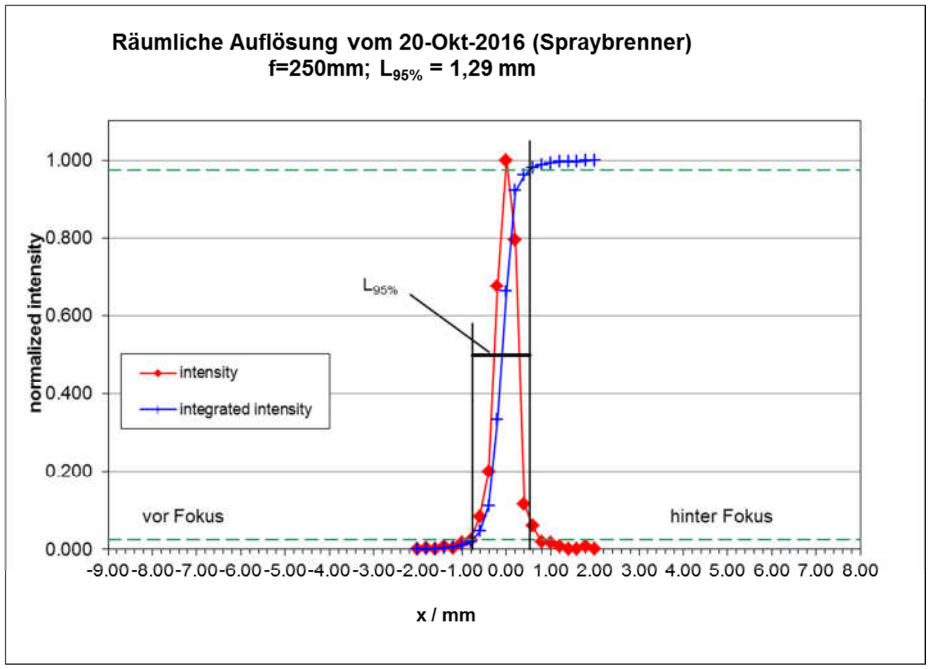

Figure 9. WIDECARS spatial resolution calculation

The test provided an intersection of the three beams of just 1.29 mm in the longitudinal direction. This result is a remarkable improvement comparing the previous SV-CARS configuration which had a 2.16 mm spatial resolution during the last test campaign (October 2017, *ECLIF Project* at HiPOT).

5. Data evaluation

All measurements were processed to obtain CARS susceptibility spectra. The preprocessing consisted of subtracting an averaged background (recorded after each run) from each single shot taken. Then, all the single shot spectra were normalized by the non-resonant spectrum (average of two Argon spectra recorded before and after each experiment) to account for the intensity distribution of the broad-band dye laser. Knowing the environmental conditions and chemical composition, theoretical spectra libraries were created. The spectral resolution of the CARS spectra depends on the instrument function which is predominantly dependent on the slit width of the spectrometer. It can be determined from an averaged room temperature air spectrum recorded during each experiment and theoretically fitted. The DLR-developed fitting code (*CARP*) iterates processed data and theoretical libraries until convergence was achieved. From the fitted spectral shape it is possible to determine the temperature. A filter can be applied to discard poorly fitted data: based on the error sum of squares, fitted spectra can be excluded from the statistical analysis whenever they exceeded an imposed value. Finally, statistical analysis can be performed for each measurement point providing mean temperature (T_{mean}), standard deviation, most probable temperature (T_{mp}), 5% and 95% confidence interval and temperature distributions. More details on the fitting code are provided by Lückerath et al.[16] The main advantage of the *CARP* code is that it is very reliable and fast to process the data. The main drawback is that only N_2 fit is possible so it would miss a lot of information once WIDECARS (or DP-CARS) is employed. Moreover the platform on which CARP is running is an *IBM-AIX* machine which is not supported anymore by the manufacturer. This made the code dependent by an out of date machine unless transferred to a different and more modern platform.

Alternative software is Sandia's *CARSFT*[17] code, particularly the modified version for DP-CARS made by Hancock et al.[18] and O´Byrne et al.[19] *CARSFT* is a *Fortran77* based code which can be used as executable on Windows platforms. It presents an internal fitting routine which is able to calculate temperature, pressure and molar fractions of the following species: N_2, O_2, CO_2, CO, and H_2. The main advantage is that is very suitable for techniques like WIDECARS or DP-CARS where spectra of multiple species are present. The main drawback is that the fitting routine was not optimized during the years and the calculation procedure is quite slow. Moreover, a multi-variable fit is not recommended since the best performances and result reliability is obtained when one variable is fit per time. This makes the software even slower in delivering results.

An improved version of *CARSFT* is the *CARSFWSC* code, developed in *Fortran90* by Cutler et al.[20], which simultaneously fits multiple species concentrations and temperature; this code calls *CARSFT* subroutines to generate theoretical spectra. So all the species present in *CARSFT* (N_2, O_2, H_2, CO, CO_2) are possible to be fit as well. The Voigt line shape model was chosen for N_2, O_2, CO, while the Galatry model was selected for H_2 as described by Magnotti et al.[21] It is also possible to fit C_2H_4 spectra but the calibration model was developed only for limited range of temperatures and concentrations.[22] The code performs faster calculations compared *CARSFT* and it was already proved to deliver reliable measurements by previous works.[9,10,11,20,21,22]

A common drawback with *CARSFT* is the unknown concentration for the non-measured species. Although this does not affect the temperature evaluation, it affects dramatically the calculation of the mole fractions: when significant unreacted components (i.e. reactant injection) or combustion minor products are present, the absolute concentration of all the fitted species are in error, since the concentration of a given species is determined as the ratio to the non-resonant susceptibility, which depends on all present species. In case one specie concentration is inaccurately fitted, then all the others are affected too, inducing a systematic error in the entire set of fitted mole fractions. To overcome this issue, a species ratio to N_2 in mole fraction can be considered a true value since the ratio of species concentration to non-resonant susceptibility is a constant value. It is recommended to use ratios to N_2, rather than other species, since large mole fractions of N_2 are always present in most of the combustion environments and the modeling of N_2 is believed to be correct. More details about the calculations are provided by Gallo et al.[10] and Cantu et al.[23]

6. Gülder burner test setup

A Gülder burner[24,25,26] was setup in the Soot Lab. The burner provides a laminar ethylene fueled diffusion flame. Two mass flow controllers (MFC) (*Bronkhorst 5850E*) were setup to control the amount of fuel and air co-flow of the burner. Ethylene fuel was employed and the respective volumetric MFC was set at 35% of the full scale, while the air co-flow's MFC was set at 10% of its full scale. A picture of the flame is shown on Figure 10.

Figure 10. Gülder's burner laminar ethylene diffusion flame in the Soot Lab

The test conditions used were chosen to replicate a previous measurement campaign by Canadian National Research Council (NRC)[27,28] and compare the results to verify the applicability and reliability of WIDECARS technique.

In particular, two different tests were performed. The first one consisted in a vertical scan of the flame with 10 mm step for each measurement. Complete WIDECARS spectra were collected using the *LaVision FlameStar2*[29] camera. Twelve hundred single shots at 10 Hz acquisition rate were recorded per measurement location and then analyzed using three different fitting codes: *CARP*, *CARSFT* e *CARSFWSC*. Only temperature out N_2 was evaluated and then compared with the CARS measurements performed by Gülder et al.[27] This test was performed to evaluate the temperature measurement reliability of both the WIDECARS technique and the fitting code.

The second test consisted in a full flame mapping. Radial scans were acquired at different height (every 5 mm) in the flame with 1 mm step. For this test a different camera was employed: *Princeton Instruments PI-MAX* equipped with HBf intensifier[30] (~50% quantum efficiency in visible range). To limit the testing time, 300 single shots per measurement were acquired at 10 Hz. The WIDECARS spectra were processed using *CARSWSC* code fitting simultaneously for temperature and N_2, O_2, and CO_2 mole fractions. All the results were compared with the simulation provided by Liu et al.[28] This test was performed to evaluate the temperature and simultaneous major specie concentration measurement reliability of both the WIDECARS technique and the *CARSFWSC* code.

7. Results of test with *LaVision FlameStar2* camera

The test with the *LaVision FlameStar2* consisted in a vertical scan in the centerline of the laminar diffusion flame. Measurements were taken at 5, 20, 30, 40, 50, 60 and 80 mm above the burner surface. Typical spectra are shown in Figure 11.

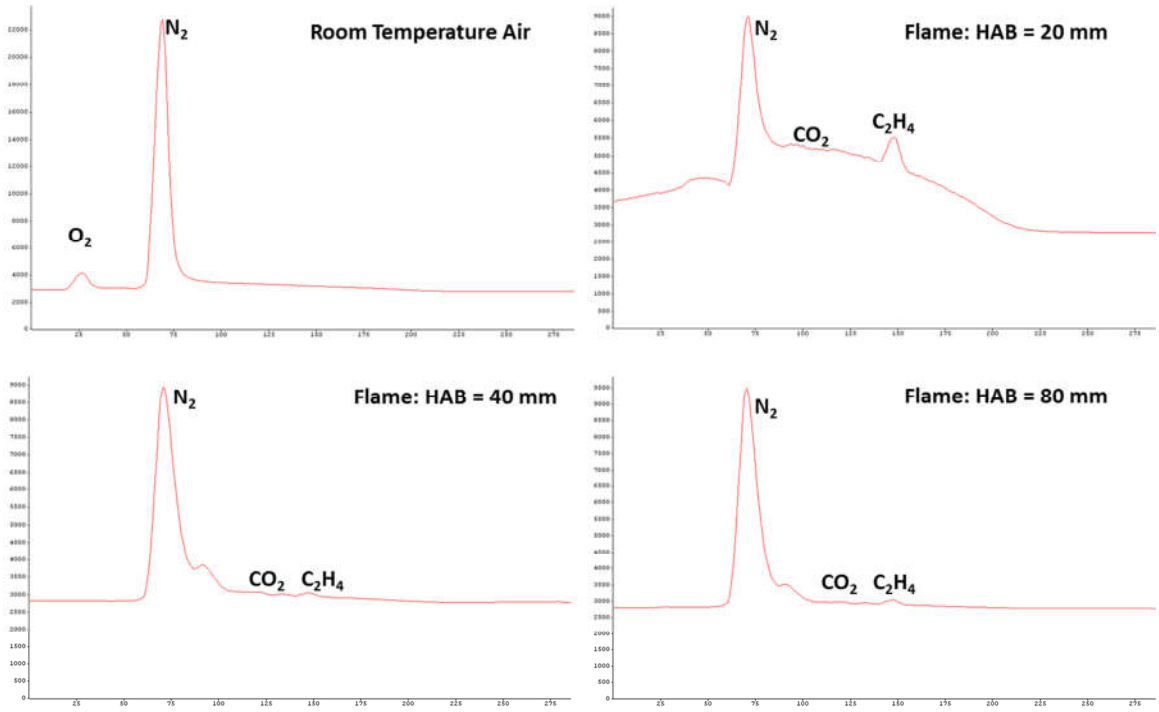

Figure 11. Typical averaged non-processed spectra

All the spectra shown are average of 1200 raw singles shots. Both vertical and horizontal scales are in arbitrary units. It can be noticed that 4 species were detected. O_2 is only present at room temperature air where no fuel was injected; then it was completed consumed once the rich combustion started. Opposite behavior can be observed for the C_2H_4: as injected it showed a strong signal (particularly at HAB = 20 mm and lower – not shown -) which influences strongly the background level due to a high value of non-resonant susceptibility (almost 4 times higher than H_2O). At HAB = 20 mm CO_2 appears as a combustion product. The CO_2 signal is quite low but it can be observed also at higher planes together with the unburned C_2H_4. N_2 is always present and the temperature was derived by its spectral shape.

All the 1200 single shots were first preprocessed (background subtraction and non-resonant curve –e.g. Argon curve – corrected) and then analyzed using three different fitting codes: *CARP*, *CARSFT* e *CARSFWSC*. Despite the fact the spectra contained information about 4 chemical species, only N_2 was considered for the fit to have a fair comparison with the N_2 CARS measurements performed at NRC and the lack of other models in *CARP*. Average temperature

was then calculated and compared with the average temperature obtained by Gülder et al.[27] using CARS at NRC in the same burner at the same conditions. Results are shown in Figure 12.

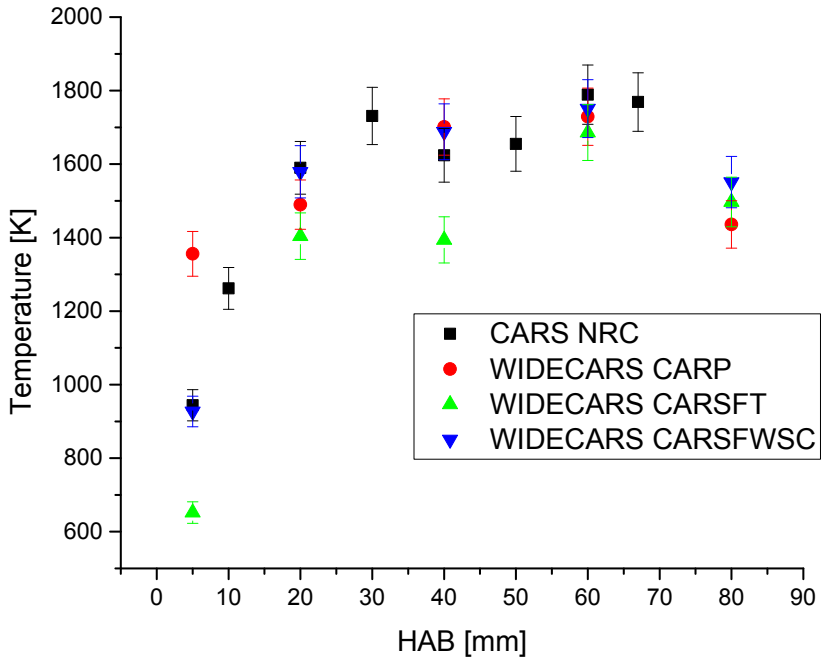

Figure 12. Comparison of temperature measurements using different fitting codes

Comparing the three fitting codes it can be observed that *CARSFWSC* is the one that agrees better with the CARS measurements at NRC. All the evaluated temperatures are located very close to the previous campaign or lie within the measurement error ($\leq$4.5%).[3]

CARP produced decent results, having the temperature almost within the instrument error, but it didn't show the same agreement as *CARSFWSC*. A possible explanation could be the strong variation in the non-resonant susceptibility coupled with the narrow region of fit. Since the code is not equipped with other chemical models except N_2, the fit was limited to a number of pixels very close the N_2 itself. This shortened the range on which the background was fit inducing some errors in the temperature evaluation. A clear example could be the point at HAB = 5 mm where the temperature is clearly overestimated.

CARSFT shows the worst results: this was expected since the code was already proven to have poor performances when more variables are fit at the same time.[17] Due to time constraints, multiple variables were fitted together and *CARFT* shoes a poor agreement with the previous campaign. However, when a single fitting variable is employed, CARSFT performs much better: this procedure is not automatized yet, so extensive coding is required in order to do not spend too much time using a manual fit.

In conclusion, *CARSFWSC* is the fitting code recommended for WIDECARS data evaluation. It shows the best agreement with the previous NRC measurements and in addition it has all the tools to further analyze multiple specie spectra. *CARP* is a good tool for temperature evaluation but it fails when multiple species are present. The lack of models for other chemical species made it a good support for other fitting codes to validate the temperature evaluation or to double check in case of dubious analysis. *CARSFT* is not recommended as a fitting code; however it is a great code to compare theory to data if the fit is conducted manually and it is a good theoretical spectra generator. For the reasons mentioned above, the data evaluation of the second test was conducted only using the *CARSFWSC* code.

8. Results of test with *Princeton Instruments PI-MAX* camera

The test with the *Princeton Instrument PI-MAX* consisted in a full radial and vertical scan of the laminar diffusion flame. Measurements were taken with a 1 mm step starting from the centerline up to 8 mm radially. Since the flame was assumed symmetric only the right side was measured. Each radial measurement was acquired at different heights above the burner surface with a step of 5 mm up to 60 mm. In addition, measurements were taken at 67 mm to match NRC last measurement position, 75 mm and 100 mm to have measurements at chemical equilibrium. Typical spectra are shown in Figure 13.

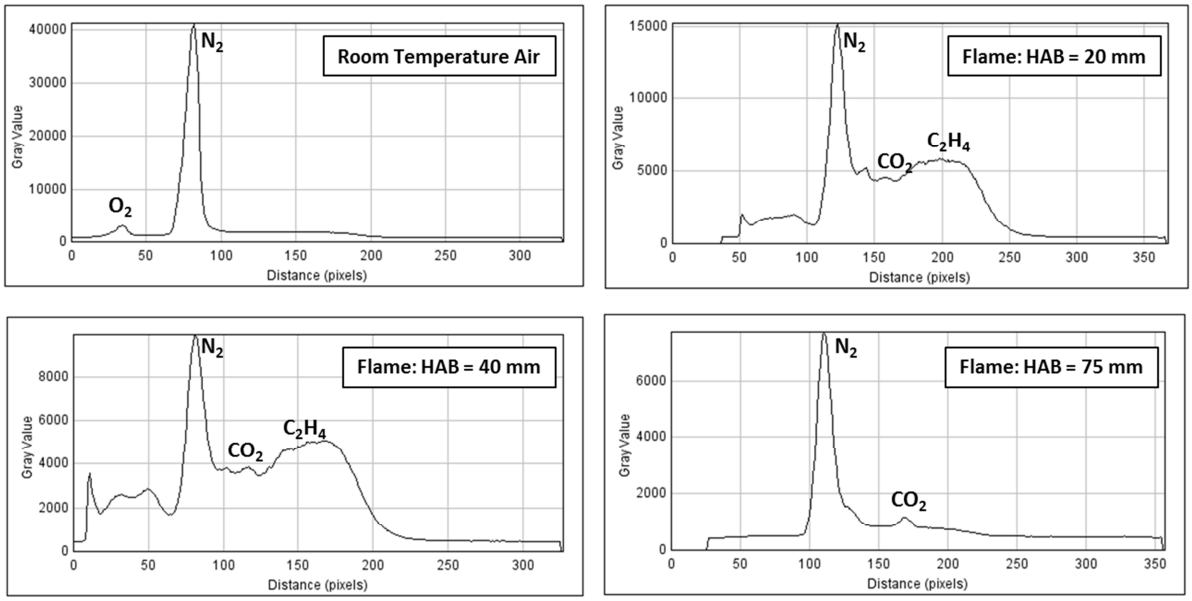

Figure 13. Typical averaged non-processed spectra

All the spectra shown are average of just 300 raw singles shots. This was done to minimize the acquisition time in order to have a complete data set of the diffusion flame. Both vertical and horizontal scales are in arbitrary units. The same considerations made in Chapter 7 are still valid for this case. In addition, it can be noticed that at HAB = 20 mm and HAB = 40 mm the influence of the C_2H_4 non-resonant susceptibility is stronger than in the previous test. This was mainly due to a shift of the broadband dye laser towards to higher wavelengths: this shift enhances the ethylene bands creating an artificial bump. This feature was corrected during the preprocessing.
All the 300 single shots were preprocessed (background subtraction and non-resonant curve – e.g. Argon curve – corrected) by dedicated macros written in java through *ImageJ*[31] *1.47t* software. This software was chosen due to its capability to import, read and process .spe format files which are the outputs of the *Princeton Instruments* devices. Then all the data were processed

using *CARSFWSC* code. The fitting parameters included temperature, horizontal shift, and molar fractions of N_2, O_2, and CO_2.

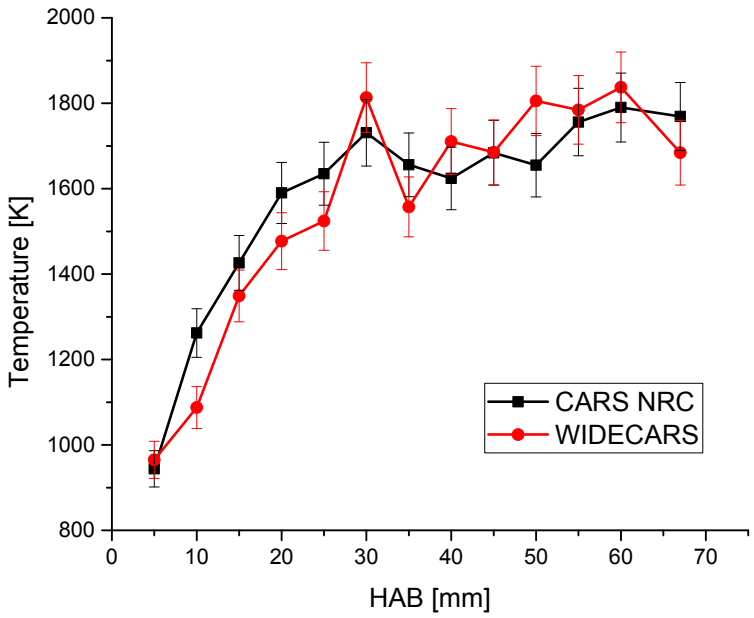

Figure 14. Comparison of temperature measurements between WIDECARS and CARS from NRC

Figure 14 shows the temperature measurements along the vertical centerline of the flame in comparison with the previous measurements performed by NRC.[28] The general behavior is similar and that gives the confidence of the repeatability of the experiment. However, some discrepancies are found. Particularly closer to the burner surface, the abundant presence of fresh C_2H_4 caused a noticeable increase of the non-resonant background: this feature is very difficult to deal with for the fitting code since the C_2H_4 model (as previously stated) was not present. This led to a rejection of several single shots and consequently to a very low statistics. Moving higher on the flame the presence of soot particles might have some interference with the background: referring back to Figure 6, the WIDECARS signal is not completely outside the C_2 Swan band interference so, when the soot production is considerable, disturbances in the spectra are expected. This interference led also to single shots rejection, hence to a low statistics that might have affected the average temperature value. However, despite the difficulties to the harsh environment, most of the points in Figure 14 are found in good agreement with the previous measurements according to the average CARS error ($\leq$4.5%, which means about ± 80 K at 1800 K). The radial measurements (not shown here) behaved similarly showing higher discrepancies in the region closer to the burner surface and where the major of the soot particles were present and converged closer to the previous CARS campaign moving away from the flame.

Concentrations measurements along with the numerical simulation values[28] are shown on Figure 15. First of all, it must be clarified that the simulations provided were not validated against any experimental values. Due to the complexity of the flame, errors in the chemical kinetics models and inaccuracies due to simplifications and/or assumptions may be possible. However, since, by author's knowledge, there are no other works available in literature about Gülder burner simulation for C_2H_4-air flame, the following discussion will consider the concentration values of Liu et al.[28]'s work as true values. Looking at Figure 15, it can be noticed that the overall trend is in agreement for all chemical species into consideration. However, some discrepancies are found. Generally, it can be noticed that there is a delay in the start of the chemical reaction in the experiment. It can be seen that after 10 mm HAB the O_2 starts decreasing meanwhile CO_2 starts forming. Contrary, CFD predicts an immediate start of the chemical reaction right after the injection (HAB = 0 mm). The same feature can be noticed looking at N_2: up to HAB = 25 mm the major discrepancies are found. Here, the abundant amount of unburned C_2H_4 dominates the chemical composition dropping the concentration values of N_2. Moreover this behavior is captured also by the temperature measurements in Figure 13 where a significant increase in temperature is found after HAB =10 mm (when chemical reaction starts according to O_2 and CO_2 concentration measurements) indicating the main presence of relatively cold unburned gases.

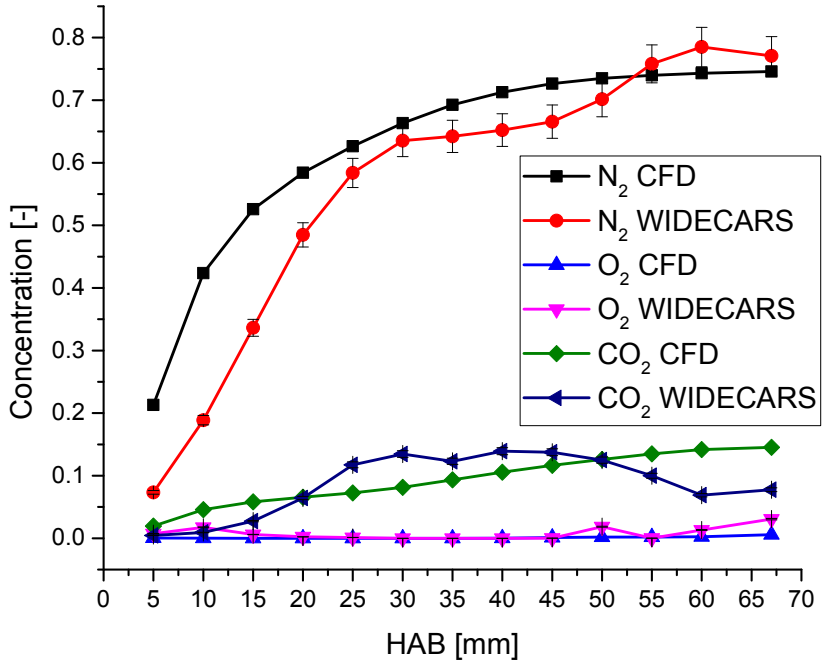

Figure 15. Comparison of specie concentration measurements between WIDECARS and numerical simulations from NRC

Moving higher (HAB between 30 and 55 mm) into the flame all the concentrations show a similar pattern. However the experimental results show lower N_2 values and a higher CO_2 values comparing to the simulation ones. This discrepancy may be explained by the presence of soot in the flame. As states before, CARS signal is not completely outside the C_2 Swan band interference so part of this disturbance may have affected the background noise. For some single shots it could be plausible that the Swan band overlapped with CO_2 band and caused an erroneous overestimation of the concentration. Consequently, N_2 may have been affected too but in a different way: the overestimation of CO_2 coupled with a disturbed (higher) background might have cause an underestimation of the concentration by the fitting code. In addition it has been noticed in some single shots a slight overlap of the second hot band of the N_2 with the fundamental band of the CO_2. This may have also been a source of underestimation of the N_2 in favor of an overestimation of CO_2.
O_2 mole fraction is the one that has the better agreement: this is explainable by the fact that in diffusion flame it is almost completed burned, hence not present in the core of the flame. This feature is well captured by the simulation and the measurements. After HAB greater than 60 mm, the WIDECARS measurements show a slightly greater amount of O_2 comparing the CFD: this could be explained by both flame fluctuations and by the length of the measurement volume. In the first case a slight fluctuation of the flame tip may lead to some single shot measured outside the flame, hence in abundance of O_2 that may affect the average concentration. In a similar way, the measurement volume is about 1.3 mm long, so more the flame shrinks, more are the possibilities that the CARS signal is generated in a mixed inside / outside flame leading to a higher average concentration in O_2.

9. Conclusions

A WIDECARS system was successfully set up for the first time at DLR-VT-Stuttgart. The mobile container including the already existing SV-CARS system was modified in order to accommodate a third laser path to perform dual pump CARS. All the modifications allow switching from SV-CARS to WIDECARS with minimal effort. The main advantages of WIDECARS with respect to SV-CARS are the possibility to simultaneously measure the main chemical species in combustion environment along with the temperature without any penalization in terms of signal strength and spatial resolution.

Since the system must be employed in sooting flames, a careful study of the CARS signal wavelength was conducted. The target was to provide a sufficient broad broad-band dye laser FWHM (at least 12 nm) to probe all the major species in combustion (N_2, CO, CO_2, O_2, H_2 and C_2H_4) and a signal away from the C_2 Swan band interference. The broad-band dye was chosen to be a mixture of DCM, Rhodamine 640 and Kiton Red: this mixture provided a FWHM of 12 nm with the peak frequency centered at 604 nm. In addition the dye was very stable and the lifetime is comparable to Rhodamine dyes. The narrowband dye laser frequency was chosen at 557 nm using Rhodamine 590 dye. This frequency allowed avoiding chemical specie overlap while fitting most of the CCD of the employed camera. These two dye-lasers together with the 532 nm generated a CARS signal of 495 nm, far enough from the main C_2 Swan band but still inside a minimal interference region. Spatial resolution of the WIDECARS configuration was tested and found to be 1.29 mm long, 1 mm shorter than the SV-CARS configuration.

Two tests were successfully conducted on a Gülder burner employing a C_2H_4-air diffusion flame. In the first test a *FlameStar2* camera was used and the temperature measurements were analyzed by three different fitting codes: *CARP*, *CARSFT*, and *CARSFWSC*. Only the vertical centerline of the flame was measured. Results were compared with previous single pump CARS measurements performed by NRC on the same burner operating at the same operating conditions. *CARSFWSC* was found to have the closest results to NRC measurements and therefore it was chosen as designated fitting code for the subsequent test. In addition, the first test demonstrated the feasibility / capability of the technique proving that all the target species were successfully probed (except CO which was left out on purpose due to the CCD size limitation) and analyzed.

In the second test a *Princeton Instruments PI-MAX* camera was used. In this second test centerline of the flame and thirteen radial scans were measured. Raw data were processed with *CARSFWSC* fitting code and each individual spectrum yielded information about temperature and specie concentrations of N_2, O_2 and CO_2. Temperature measurements were again compared with NRC ones. As before, the temperature measurements were in agreement with the previous campaign; for this test, more points were evaluated and most of them lay inside the CARS measurement error interval. Discrepancies were found only closer to the fuel injection where the large amount of unburned C_2H_4 was present. This caused an increase of the non-resonant susceptibility that may have affected the temperature evaluation. Since no other experimental data were available, concentration values were compared with numerical simulations by NRC on the same burner

operating at the same operating conditions. However, numerical simulations were not validated against experimental data before, so any possible source of modelling error cannot be taken into account in this report. Concentration comparison shows a similar trend for all the chemical species into consideration. However discrepancies are found for N_2 and CO_2. The first one shows an underestimation of the concentration in the N_2 while the second one shows an overestimation comparing to the numerical simulations. It is still not clear the source of these differences, but the soot presence may have caused an increase in the non-resonant susceptibility that could have caused some fitting error. Another cause may have been the slight overlap of the N_2 second hot band with the fundamental band of CO_2: this could have affected the fitting routine as well. O_2 is in a good agreement with simulation. O_2 measurements together with CO_2 identify the start of the chemical reaction: this point is few millimeters higher above the burner surface compared to the numerical simulations indicating a small time delay between the experiment and the theoretical calculations.

10. Future developments and recommendations

The results of the first set of tests employing WIDECARS were really encouraging and proved the feasibility and reliability of the technique in sooting flames environment. However, some discrepancies with the previous campaign performed by NRC and numerical simulation may suggest some more investigations to improve the precision and the capability of the instrument and/or minimize/correct some possible error sources.

The main component which it should be focused on is the FWHM of the broad-band dye laser. In this first attempt the optimization of the dye was limited by the CCD size, hence to just 12 nm. However, due to the confirmed purchase (on January 2019) of the new detection system (*LaVison Intensified NanoStar*), a new study is recommended to exploit the full capability of the camera. Avoiding replicating the already attempted dye mixture, a promising possibility would be mixing DCM Special (a modification of DCM dye with the peak centered at 620 nm) with Rhodamine 640 (and eventually Kiton Red). This solution is similar to the one tested and used for this report but DCM Special is shifted more to the blue comparing regular DCM: this may preserve a wider FWHM while mixed with the Rhodamine dye. Another possibility is to use the mixture Pyrromethene 597 and Pyrromethene 650 as suggested by Gallo et al.: this dye was already discussed in this report and discarded because of a poor lifetime. However, the FWHM of 23 nm could be sufficiently advantageous over the fast dye degradation, if no other mixtures can provide similar features.

The narrow-band dye laser may have to be changed as well following the changes of the broad-band in order to guarantee a CARS signal outside the C_2 Swan band interference. On this matter, it would be preferable to obtain the CARS signal more towards the blue, in the range of 485 nm. On the other hand the extension of the CCD size may allow detecting the chemical species that were on purpose left out of the camera view. Here CO and H_2 may be possible to appear in the field of view implying some changes of the narrow-band dye laser frequency to avoid specie overlap.

It is also recommended to enable the seed for the pumping laser beam. This feature was not available for the reported test since the seeder of the Nd:YAG was not working properly. A *Spectra Physics* service was performed on March 2019 and the seeder was repaired, fully re-aligned and again in operation. Using a seeded pump source sharpens the 532 nm laser linewidth yielding a higher resolution of the spectral lines. In this way more rotational lines may be present in the measurements improving the accuracy of the fitting *CARSFWSC* code.

Finally, it is recommended to repeat the Gülder burner test reported to compare the old configuration and the previous measurements and numerical simulations against the new one. In addition, it is suggested to perform a similar test on a more well-studied burner (for example like a McKenna burner) in order to have more literature available to compare the results with.

11. References

[1] P. D. Maker, R. W. Terhune, "Study of Optical Effects Due to an Induced Polarization Third Order in the Electric Field Strength", *Applied Physics Letters*, Vol. 23, pp. 240-242, 1973

[2] A. C. Eckbreth, "Laser Diagnostics for Combustion Temperature and Species 2nd Ed", Combustion Science & Technology Book Series, Vol. 3, Taylor & Francis, New York NY, USA, 2002

[3] L. M. L. Cantu, J. Grohmann, W. Meier, M. Aigner, „Temperature measurements in Confined Swirling Spray Flames by Vibrational Coherent Anti-Stokes Spectroscopy", *Experimental Thermal and Fluid Science*, Vol. 95, pp. 52-59, 2018

[4] K. P. Geigle, Y. Schneider-Kühnle, M. S. Tsurikov, R. Hadef, R. Lückerath, V. Krüger, W. Stricker, M. Aigner, "Investigation of Laminar Flames for Soot Model Validation Using SV-CARS and LII", *Proceeding Combustion Institute*, Vol. 30, pp. 1645-1653, 2005

[5] R. P. Lucht, "Three-laser Coherent Anti-Stokes Raman Scattering Measurements of Two Species", *Optic Letters*, Vol. 12, No. 2, pp. 78-80, 1987

[6] A. Malarski, F. Beyrau, A. Leipertz, „Interference effects of C_2-Radicals in Nitrogen Vibrational CARS Thermometry Using a Frequency-Doubled Nd:YAG Laser*", Journal of Raman Spectroscopy*, Vol. 36, Issue 2, 2004

[7] D. V. Flores, "Analysis of Lean Premixed Turbulent Combustion Using Coherent Anti-Stokes Raman Spectroscopy Temperature Measurements" Doctor of Philosophy Dissertation, Department of Chemical Engineering Brigham Young University, Provo UT, USA, April 2003

[8] S. A. Tedder, J. L. Wheeler, P. M. Danehy, "Width-Increased Dual-Pump Enhanced Coherent Anti-Stokes Raman Spectroscopy (WIDECARS)", *Optical Society of America*, Vol. 49, Issue 8, pp. 1305-1313, 2009

[9] E. C. A. Gallo, L. M. L. Cantu, A. D. Cutler, "Width Increased Enhanced Coherent Anti-Stokes Raman Spectroscopy Measurements of Major Species Concentrations and Temperature in an Air-Ethylene Flame*", 30th AIAA Aerodynamic Measurement Technology and Ground Testing Conference*, AIAA AVIATION Forum, AIAA 2014-2525, 2014

[10] E. C. A. Gallo, "Simultaneous Measurements of Temperature and Major Specie Concentration in a Hydrocarbon-Fueled Dual-Mode Scramjet Using WIDECARS", Doctor of Philosophy

Dissertation, Department of Mechanical and Aerospace Engineering, The George Washington University, Washington DC, USA, January 2016

[11] E. C. A. Gallo, L. M. L. Cantu, A. D. Cutler, R. D. Rockwell, C. P. Goyne, J. C. McDaniel, "WIDECARS Measurements of a Premixed Ethylene-Air Flame in a Small-Scale Dual-Mode Scramjet Combustor", *54th AIAA Aerospace Sciences Meeting*, AIAA SciTech Forum, AIAA 2016-0656, 2016

[12] U. Brackmann, "Lambdachrome Laser Dyes 3rd Edition", Lambda Physik, Göttingen, Germany, 2000

[13] Exciton Inc., "Exciton Tuning Curves", Dayton OH, USA, www.exciton.com

[14] Sirah Lasertechnik GmbH, "Laser Dyes 532 nm", Grevenbroich, Germany, www.sirah.com

[15] Sirah Lasertechnik GmbH,"Sirah Pulsed Dye Laser Service Manual", Grevenbroich, Germany, www.sirah.com, 2005

[16] R. Lückerath, M. Woyde, W. Meier, W. Stricker, U. Schnell, H. C. Magel, J. Görres, H. Spliethoff, H. Maier, "Comparison of Coherent Anti-Stokes Raman-Scattering Thermometry with Thermocouple Measurements and Model Prediction in Both Natural-Gas and Coal-Dust Flames", *Applied Optics,* Vol. 34, pp. 3303-3312, 1995

[17] R. E. Palmer, "The CARSFT Computer Code for Calculating Coherent Anti-Stokes Raman Spectra: User and Programmer Information", Sandia report SAND89-8206, 1989

[18] R. D. Hancock, F. R. Schauer, R. P. Lucht, R. L. Farrow, "Dual-Pump Coherent Anti-Stokes Raman Scattering Measurements of Nitrogen and Oxygen in a Laminar Diffusion Flame", *Applied Optics*, Vol. 36, Issue 15, 1997

[19] S. O'Byrne, P. M. Danehy, S. A. Tedder, A. D. Cutler, "Dual-Pump Coherent Anti-Stokes Raman Scattering in a Supersonic Combustor", *AIAA Journal*, Vol. 45, Issue 4, pp. 922.933, 2007

[20] A. D. Cutler , G. Magnotti, "CARS Spectral Fitting with Multiple Resonant Species Using Sparse Libraries", *Journal of Raman Spectroscopy*, Vol.42, Issue 11, pp.1949-1957, 2011

[21] G. Magnotti, A.D. Cutler, P. M. Danehy, "Development of a dual-pump coherent anti-Stokes Raman spectroscopy system for measurements in supersonic combustion" *Applied Optics*, Volume 52, Issue 20, pp. 4779-4791, 2013

[22] A. D. Cutler, E. C. A. Gallo, L. M. L. Cantu, "Coherent Anti-Stokes Raman Spectroscopy Measurement of Ethylene in Combustion", *Applied Optics*, Vol. 56, Issue 11, pp. E30-E36, 2017

[23] L. M. L. Cantu, E. C. A. Gallo, A. D. Cutler, P. M. Danehy, "Dual-pump CARS of Air in a Heated Pressure Vessel up to 55 Bar and 1300 K", *52nd Aerospace Sciences Meeting*, AIAA SciTech Forum, AIAA 2014-1098, 2014

[24] Ö. L. Gülder, D. R. Snelling, R. A. Sawchuck, "Influence of Hydrogen Addition to Fuel on Temperature Field and Soot Formation in Diffusion Flames", *The Combustion Institute*, pp. 2351-2358, 1996

[25] D. R. Snelling, K. A. Thomson, H. Guo, G. J. Smallwood, Ö. L. Gülder, E. J. Weckman, R. A. Fraser, "Spectrally Resolved Measurement of Flame Radiation to Determine Soot Temperature and Concentration", *AIAA Journal*, Vol. 40, Issue 9, pp. 1789-1795, 2002

[26] R. Hadef, K. P. Geigle, J. Zerbs, R. A. Sawchuck, D. R. Snelling, "The Concept of 2D gated Imaging for Paricle Sizing in a Laminar Diffusion Flame", *Applied Physics B*, Vol. 112, pp. 395,408, 2013

[27] Ö. L. Gülder, K. A. Thomson, D. R. Snelling, „Influence of the Fuel Nozzle Material on Soot Formation and Temperature Field in Coflow Laminar Diffusion Flames", The Combustion Institute Canadian Section, Spring 200 Technical Meeting, University of Ottawa, 2000

[28] F. Liu, H. Guo, G. J. Smallwood, Ö. L. Gülder, "Effects of Gas and Soot Formation in a Coflow Laminar Ethylene Diffusion Flame", *Journal of Quantitative Spectroscopy & Radiative Transfer*, Vol. 73, pp. 409-421, 2002

[29] LaVision GmbH, "FlameStar 2 Camera System – Operational Manual", Göttingen Germany, 1998

[30] Princeton Instruments Inc., "PI-MAX Camera User Manual, Version 3.A", Trenton NJ, USA, 2001

[31] W. S. Rasband, ImageJ, US National Institute of Health, Bethesda MD, USA, http://rsb.info.nih.gov/ij, 1997-2009.